American Journal of Pathology, Vol. 167, No. 3, September 2005

Stem Cells, Tissue Engineering and Hematopoietic Elements

Mast Cell-Deficient *W-sash* c-*kit* Mutant *Kit*$^{W\text{-}sh/W\text{-}sh}$ Mice as a Model for Investigating Mast Cell Biology *in Vivo*

Michele A. Grimbaldeston,* Ching-Cheng Chen,* Adrian M. Piliponsky,* Mindy Tsai,* See-Ying Tam,* and Stephen J. Galli*†

From the Departments of Pathology and Microbiology and Immunology,† Stanford University School of Medicine, Stanford, California*

Mice carrying certain mutations in the *white spotting* (*W*) locus (ie, c-*kit*) exhibit reduced c-*kit* tyrosine kinase-dependent signaling that results in mast cell deficiency and other phenotypic abnormalities. The c-*kit* mutations in *Kit*$^{W/W\text{-}v}$ mice impair melanogenesis and result in anemia, sterility, and markedly reduced levels of tissue mast cells. In contrast, *Kit*$^{W\text{-}sh/W\text{-}sh}$ mice, bearing the *W-sash* (*W*^{sh}) inversion mutation, have mast cell deficiency but lack anemia and sterility. We report that adult *Kit*$^{W\text{-}sh/W\text{-}sh}$ mice had a profound deficiency in mast cells in all tissues examined but normal levels of major classes of other differentiated hematopoietic and lymphoid cells. Unlike *Kit*$^{W/W\text{-}v}$ mice, *Kit*$^{W\text{-}sh/W\text{-}sh}$ mice had normal numbers of TCR$\gamma\delta$ intraepithelial lymphocytes in the intestines and did not exhibit a high incidence of idiopathic dermatitis, ulcers, or squamous papillomas of the stomach, but like *Kit*$^{W/W\text{-}v}$ mice, they lacked interstitial cells of Cajal in the gut and exhibited bile reflux into the stomach. Systemic or local reconstitution of mast cell populations was achieved in non-irradiated adult *Kit*$^{W\text{-}sh/W\text{-}sh}$ mice by intravenous, intraperitoneal, or intradermal injection of wild-type bone marrow-derived cultured mast cells but not by transplantation of wild-type bone marrow cells. Thus, *Kit*$^{W\text{-}sh/W\text{-}sh}$ mice represent a useful model for mast cell research, especially for analyzing mast cell function *in vivo*. *(Am J Pathol 2005, 167:835–848)*

Genetically mast cell-deficient c-*kit* mutant mice have become a powerful tool for identifying and quantifying the contributions of mast cells in many biological responses *in vivo*. Mice carrying spontaneous loss-of-function mutations at both alleles of the dominant *white spotting* (*W*) locus (ie, c-*kit*), exhibit a marked reduction in c-*kit* tyrosine kinase-dependent signaling, resulting in disrupted normal mast cell development and survival,[1,2] and therefore mast cell function, as well as many other phenotypic abnormalities that are unrelated to the mast cell deficiency.[3–5]

Several different *W* mutant rodents have been investigated as potential models for the analysis of mast cell function *in vivo*, including *Kit*$^{W/W\text{-}v}$ and *Kit*$^{W\text{-}f/W\text{-}f}$ mice and *Kit*$^{W\text{-}s/W\text{-}s}$ rats.[1,6,7] In general, the utility of these animals as models in which to investigate mast cell function depends on both the extent of their mast cell deficiency and the nature and extent of their other c-*kit*-related phenotypic abnormalities. The WBB6F$_1$-*Kit*$^{W/W\text{-}v}$ mouse is currently the most commonly used animal model for such investigations. *Kit*$^{W/W\text{-}v}$ mice are profoundly mast cell-deficient; the adult mice contain no detectable mast cell populations in the peritoneal cavity, gastrointestinal tract, respiratory system, heart, brain, skeletal muscle, spleen, and multiple other anatomical sites, and they exhibit $<1\%$ of the wild-type levels of skin mast cells by the time they reach 6 to 8 weeks of age.[1] However, the reduced c-*kit* function in these mice results in many other phenotypic abnormalities, including a macrocytic anemia, sterility, impaired melanogenesis, a virtual lack of interstitial cells of Cajal (ICC), and a decline in the number of intestinal TCR$\gamma\delta$ intraepithelial lymphocytes (IELs) with age.[8–12] *Kit*$^{W/W\text{-}v}$ mice also develop a high incidence of spontaneous dermatitis,[13] squamous papillomas of the forestomach,[14] gastric ulcers,[15] and dilatation of the duodenum.[16]

The *W-sash* mutation, which arose spontaneously in a cross between two inbred strains of mice (C3H/HeH $\times$ 101/H), was first described 23 years ago.[17] However,

Supported by the Australian National Health and Medical Research Council (C.J. Martin fellowship to M.A.G.) and the United States Public Health Service (grants AI23990, CA72074, and HL67674, project 1 to S.J.G.).

Accepted for publication May 17, 2005.

The authors have no conflicting financial interests.

Address reprint requests to Stephen J. Galli, Department of Pathology, L-235, Stanford University School of Medicine, 300 Pasteur Dr., Stanford, CA 94305-5324. E-mail: sgalli@stanford.edu.

C57BL/6-*Kit*$^{W\text{-}sh/W\text{-}sh}$ mice only recently have begun to be used as a model for studies of mast cell function *in vivo*.[18] *W-sash* (*W*^{sh}) is an inversion mutation in the transcriptional regulatory elements upstream of the *c-kit* transcription start site on mouse chromosome 5.[19] Earlier work indicated that the *W*^{sh} mutation results in fewer developmental abnormalities than do those c-*kit/W* mutations which are null mutations or alter the c-*kit* coding region and thereby cause varying degrees of impairment of intrinsic c-*kit* receptor function. For example, until very recently, the only reported phenotypic abnormalities in *Kit*$^{W\text{-}sh/W\text{-}sh}$ mice were an impairment of skin pigmentation and a mast cell-deficiency in the skin and peritoneal cavity.[18,20–23] Subsequently, it was reported that adult (10 weeks old) *Kit*$^{W\text{-}sh/W\text{-}sh}$ mice are mast cell-deficient in multiple anatomical sites.[24] Moreover, *Kit*$^{W\text{-}sh/W\text{-}sh}$ mice, unlike *Kit*$^{W/W\text{-}v}$ mice, are fertile (with appreciable numbers of germ cells in their gonads) and are not anemic.[17,20] Accordingly, *Kit*$^{W\text{-}sh/W\text{-}sh}$ mice may have advantages for some mast cell studies, compared to the *Kit*$^{W/W\text{-}v}$ and *Kit*$^{W\text{-}f/W\text{-}f}$ mutants. Although recent studies demonstrate that *Kit*$^{W\text{-}sh/W\text{-}sh}$ mice can be transplanted successfully with bone marrow-derived mast cells,[18,24] a detailed comparison of the phenotypic aberrations that are observed in mice carrying the *Kit*$^{W/W\text{-}v}$ or *Kit*$^{W\text{-}sh}$ mutant alleles has not yet been reported.

In the present study, we assessed the effects of the *W*^{sh} mutation on the development of multiple different cell lineages, including mast cells, basophils, and other hematopoietic and lymphoid cells, and ICC, and on the incidence of certain types of pathology that have been reported in *Kit*$^{W/W\text{-}v}$ mice. Our results show that adult *Kit*$^{W\text{-}sh/W\text{-}sh}$ mice are profoundly mast cell-deficient in all tissues compared with age-matched wild-type littermates, and that the heterozygous (*Kit*$^{+/W\text{-}sh}$) mice exhibit a mild mast cell deficiency in certain anatomical sites. Moreover, we demonstrate that *Kit*$^{W\text{-}sh/W\text{-}sh}$ mice can accept transplantation of genetically compatible bone marrow-derived cultured mast cells (BMCMCs) with normal c-*kit* expression, by adoptive transfer of these cells via intraperitoneal, intradermal, or intravenous injection, without the development of other donor-derived hematopoietic cells. And even though *Kit*$^{W\text{-}sh/W\text{-}sh}$ mice lacked ICC and demonstrated significant bile reflux into the stomach, the levels of hematopoietic cells (other than mast cells) and lymphoid cells, including TCR$\gamma\delta$ IELs, were normal in adult *Kit*$^{W\text{-}sh/W\text{-}sh}$ mice, and these animals did not exhibit a high incidence of spontaneous pathology affecting the skin, stomach, or duodenum.

Materials and Methods

Mice

Mast cell-deficient *Kit*$^{W\text{-}sh/W\text{-}sh}$, C57BL/Ka-Thy1.1-CD45.1 (Ly5.2), and green fluorescent protein (GFP)-expressing C57BL/Ka-Thy1.1-CD45.2 (Ly5.1) mice were bred and maintained at the Stanford University Research Animal Facility. *Kit*$^{W\text{-}sh/W\text{-}sh}$ mice on the C57BL/6 background were generously provided by Dr. Peter Besmer (Molecular Biology Program, Memorial Sloan-Kettering Cancer Center and Cornell University Graduate School of Medical Sciences, New York, NY).[21] β-Actin/enhanced green fluorescent protein (eGFP) transgenic mice on the C57BL/Ka-Thy1.1-CD45.2 (Ly5.1) background were generated as previously described using the pCXEGFP vector,[25] and allowed to freely imbibe acidified water (pH 2.5). Female 6-week-old WBB6F$_1$-*Kit*$^{W/W\text{-}v}$ mice and their wild-type littermates were obtained from Jackson Laboratories (Bar Harbor, ME). All experiments were performed in compliance with the Guide for the Care and Use of Laboratory Animals prepared by the Institute of Laboratory Animal Resources, National Research Council, and published by the National Academy Press (revised 1996) and the Stanford University Committee on Animal Welfare.

Preparation and Adoptive Transfer of BMCMCs into Mast Cell-Deficient Mice

Bone marrow cells from female *Kit*$^{+/+}$ (C57BL/6-Ly5.1 wild-type littermates, or C57BLKa-Ly5.2, or β-act-eGFP-C57BLKa-Ly5.1) mice were cultured in Dulbecco's modified Eagle's medium (DMEM) (Sigma Chemical Co., St. Louis, MO) supplemented with 20% WEHI-3 conditioned medium (as a source of IL-3) for 4 to 6 weeks, at which time >95% of the cells were identified as BMCMCs by May Grunwald-Giemsa staining and by flow cytometric analysis (for details, see Supplementary Methods at *http://ajp.amjpathol.org*). For mast cell reconstitution studies, BMCMCs were transferred by intradermal (1×10^6 cells in 40 μl of DMEM/ear, or 4×10^6 cells in 8×50-μl aliquots in two rows down the length of shaved back skin), or by intraperitoneal (2.5 to 5×10^6 cells in 200 μl of DMEM), or by tail-vein or retro-orbital intravenous (1×10^7 cells in 200 μl of DMEM) injection into 4-week-old female *Kit*$^{W\text{-}sh/W\text{-}sh}$ mice. Six to eight weeks after intradermal or intraperitoneal transfer, or 12 weeks after intravenous injection, mice were sacrificed and tissues were assessed for repair of mast cell deficiency.

Bone Marrow Transplantation

Bone marrow cells were collected from femurs of wild-type littermates (C57BL/6-Ly5.1) and C57BL/Ka-Thy1.1-CD45.1 (Ly5.2). Red blood cells were lysed with 1 ml of ACK lysis buffer (Cambrex Bioscience, Walkersville, MD) for 5 minutes, and the remaining whole bone marrow (WBM) cells centrifuged at 1200 rpm for 5 minutes, and then resuspended in 1× phosphate-buffered saline (PBS) for injection. Female 4- to 6-week-old *Kit*$^{W\text{-}sh/W\text{-}sh}$ mice were injected intraperitoneally or intravenously (retro-orbital) with 1×10^6 WBM cells (from femurs) in 200 μl of PBS, or 1×10^7 WBM cells in 100 μl of PBS, respectively. Some recipient *Kit*$^{W\text{-}sh/W\text{-}sh}$ mice were lethally irradiated with a split dose of 950 rad to facilitate the bone marrow reconstitution, as described.[26] For irradiated mice receiving 1×10^7 Ly5.2-expressing BMCMCs intravenously, a radioprotective dose of 3×10^5

WBM cells obtained from $Kit^{+/+}$-Ly5.1 colony littermates was transferred simultaneously.

Flow Cytometric Analysis of Hematopoietic Lineages

Cells were blocked with unconjugated anti-FcγRII/III (2.4G2; BD Pharmingen, San Diego, CA) then stained with PE/Cy7-conjugated anti-CD45.1 (A20; eBioscience, San Diego, CA) and a combination of PE- or APC-labeled antibodies specific for B220 (6B2), CD3 (145-2C11), CD4 (GK1.5), CD8 (53-6.7), CD11c (N418), F4/80 (BM8), Gr-1 (8C5), FcϵRIα (MAR-1), CD49b (DX5), and CD117. Cells were analyzed by using a triple laser (407-nm krypton laser, 488-nm argon laser, and 598-nm dye laser) FACS Vantage SE/DiVa (Becton Dickinson, Mountain View, CA).

Staining and Quantification of Mast Cells

Mice were euthanized and samples of back skin, ear pinna, tongue, lung, spleen, trachea, heart, stomach, jejunum, ileum, colon, kidney, bladder, tail, liver, brain, and lymph nodes (submaxillary, axillary, and inguinal) were fixed in 10% buffered formalin, embedded in paraffin ensuring a cross-sectional orientation of all tissues, and 4-μm sections were cut. Mesenteric windows were arranged onto slides and fixed for 1 hour in Carnoy's solution (3:2:1 v/v/v of ethanol, chloroform, and acetic acid). All tissues, with the exceptions of ear pinna and brain, were stained with Csaba stain for mast cell detection.[27] Csaba stain contains both safranin (red, identifying mature mast cells) and alcian blue (blue, identifying less mature mast cells), which bind to mast cell granules. For ear and brain sections, mast cells were stained metachromatically with 0.1% toluidine blue, pH 1 (cytoplasmic granules appear purple). Mast cells were quantified according to area (mm^2) or expressed in numbers per mm horizontal field length (back skin and ear pinna) using computer-generated image analysis (NIH Image J software, version 1.29×) (for details, see Supplementary Methods at *http://ajp.amjpathol.org*).

Immunohistochemical Detection of ICC

Samples of freshly dissected stomach, ileum, and colon were gently flushed in PBS to remove luminal contents, and prepared for cryopreservation as previously described.[28,29] Briefly, tissues were treated with a series of graded sucrose solutions (5%, 10%, 15%, and 20% sucrose in PBS) for 20 to 30 minutes each on ice, and embedded overnight at 4°C in a solution consisting of OCT (Tissue Tek, IL) and 20% sucrose in PBS (1 part/2 parts; v/v). Tissues were then embedded in OCT ensuring a cross-sectional orientation and rapidly frozen on dry ice. Frozen sections (10 μm) were cut and fixed in ice-cold acetone for 2 to 5 minutes. After incubation with 10% normal rabbit serum for 30 minutes at room temperature, sections were treated overnight at 4°C with 0.6 μg/ml goat polyclonal anti-c-*kit* IgG (sc-1494; Santa Cruz Biotechnology, Santa Cruz, CA). Immunoreactivity was detected with a 1:40 dilution of fluorescein isothiocyanate-conjugated rabbit anti-goat IgG (DAKO, Carpinteria, CA) incubated for 2 hours at room temperature. Control tissues were prepared in a similar manner but with the omission of the primary antibody. Images were captured using a confocal microscope (Eclipse TE300; Nikon, Melville, NY) with an excitation wavelength for fluorescein isothiocyanate fluorescence (488 nm), and LaserSharper2000, version 5.2, software. For detection of ICC in the stomach and ileum of 7-day-old, 14-day-old, and 4-week-old C57BL/6-$Kit^{+/+}$ and $Kit^{W\text{-}sh/W\text{-}sh}$ mice (Supplementary Figure 1 at *http://ajp.amjpathol.org*), a *Z*-series of up to 11 images through a depth of 10 μm were collected and merged to form a confocal micrograph.

Measurement of Bile Acids in the Stomach

Mutant mice of the $Kit^{W\text{-}sh/W\text{-}sh}$ and $Kit^{W/W\text{-}v}$ genotypes, together with their respective wild-type littermates were assessed for stomach concentrations of total bile acids 7 days, 4 to 6 weeks, and 10 to 14 weeks after birth, as previously described.[30] Briefly, mice were starved for 6 hours, euthanized, and the stomachs ligated at the distal (anal) and proximal (oral) ends, and then removed. Distilled water (0.7 ml) was injected into each stomach with a syringe and needle, and the gastric contents were collected after gentle pipetting. The pH of the gastric contents was corrected to the range of pH 6.5 to 7.5 and all samples were adjusted to 1 ml with addition of distilled water. The concentration of total bile acids of each sample was measured using a bile acids kit (Trinity Biotech USA, MO). Bile acids are first oxidized to 3-oxo bile acids with the catalytic enzyme 3α-hydroxysteroid dehydrogenase. During this reaction an equimolar quantity of nicotinamide adenine dinucleotide (NAD) is reduced to nicotinamide adenine dinucleotide (NADH). The NADH is subsequently oxidized to NAD with concomitant reduction of nitro blue tetrazolium salt to formazan by the catalytic action of diaphorase. The color of the resulting diformazan was measured at 530 nm with a spectrophotometer. The intensity of the color produced is directly proportional to the bile acid concentration in the sample. The concentration of total bile acids in the samples was calculated using a bile acids calibrator (Trinity Biotech USA), in which the difference in absorption between the test and blank reagents of each sample was divided by the difference in absorption between the test and blank reagents of the calibrator, and the resulting value multiplied by the concentration of the calibrator to yield gastric content bile acid concentration, expressed as μmol/L. Quality control of each assay and between assays was monitored with the inclusion of control sera with known bile acids concentration (bile acids control set, Trinity Biotech USA). Eight assays were performed and the mean ± SD together with the coefficient of variation (percent) of the calibrator, normal control serum, and abnormal control serum, were 0.405 ± 0.015 (3.7%), 6.61 ± 0.38 (5.7%), and 40.02 ± 1.8 (4.5%), respectively.

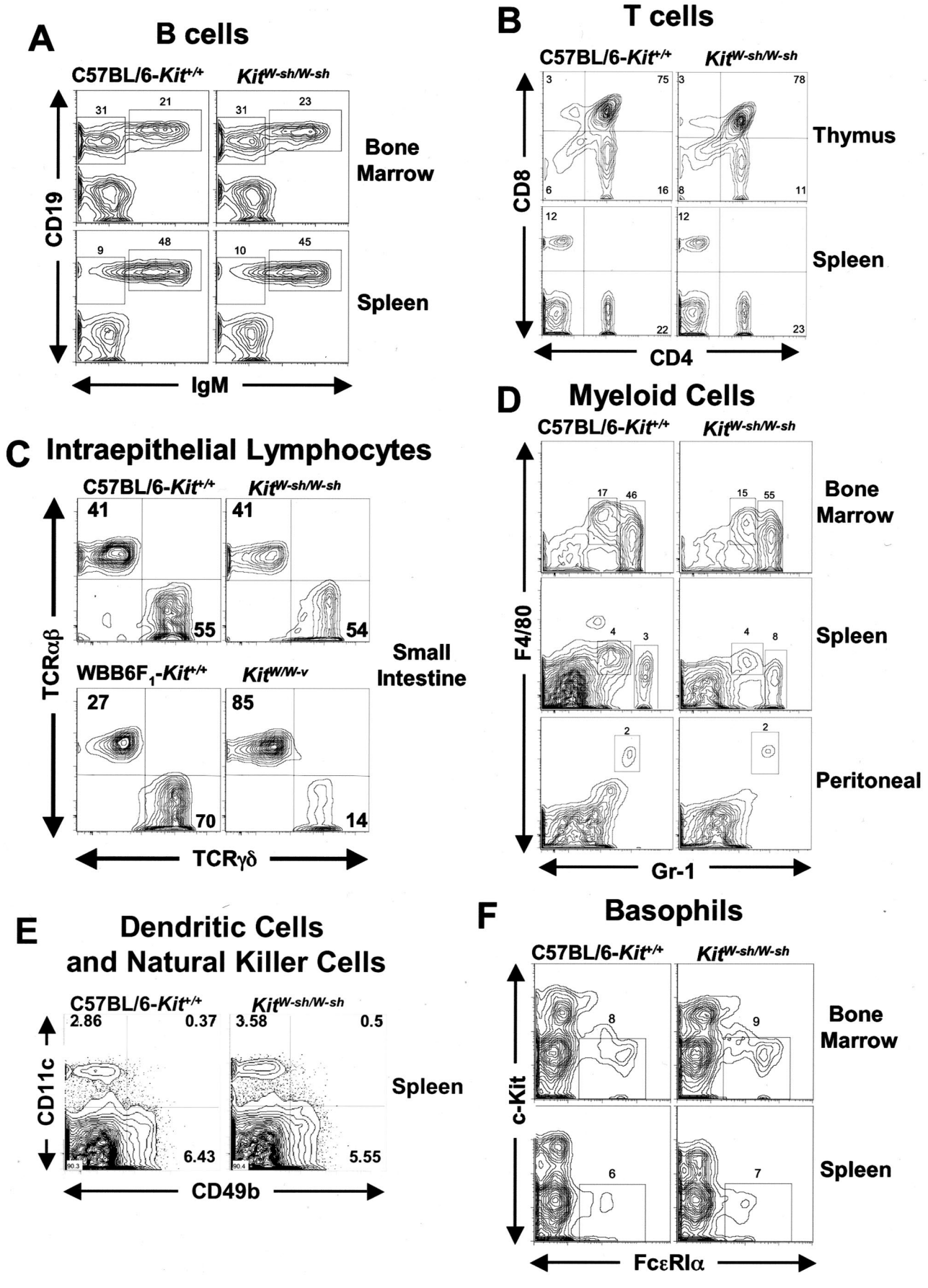
A
B cells
C57BL/6-Kit+/+
Kit W-sh/W-sh
31
21
31
23
Bone Marrow
9
48
10
45
Spleen
CD19
IgM
B
T cells
C57BL/6-Kit+/+
Kit W-sh/W-sh
3
75
3
78
Thymus
6
16
8
11
12
12
Spleen
22
23
CD8
CD4
C
Intraepithelial Lymphocytes
C57BL/6-Kit+/+
Kit W-sh/W-sh
41
41
55
54
Small Intestine
WBB6F1-Kit+/+
Kit W/W-v
27
85
70
14
TCRαβ
TCRγδ
D
Myeloid Cells
C57BL/6-Kit+/+
Kit W-sh/W-sh
17
46
15
55
Bone Marrow
4
3
4
8
Spleen
2
2
Peritoneal
F4/80
Gr-1
E
Dendritic Cells and Natural Killer Cells
C57BL/6-Kit+/+
Kit W-sh/W-sh
2.86
0.37
3.58
0.5
Spleen
6.43
5.55
CD11c
CD49b
F
Basophils
C57BL/6-Kit+/+
Kit W-sh/W-sh
8
9
Bone Marrow
6
7
Spleen
c-Kit
FcεRIα

Statistics

A multiple comparison procedure using an analysis of variance and Fisher's test was used to determine statistical significance between groups ($n = 3$ to 16 mice/group). Probabilities ≤ 0.05 were considered significant.

Results

Hematopoietic and Lymphoid Cell Populations

Adult $Kit^{W\text{-}sh/W\text{-}sh}$ mice displayed normal levels of B cells in bone marrow and spleen (Figure 1A); T cells in thymus and spleen (Figure 1B); myeloid cells (granulocytes and macrophages) in bone marrow, spleen, and peritoneal cavity (Figure 1D); dendritic cells and natural killer cells in the spleen (Figure 1E); and basophils in bone marrow and spleen (Figure 1F). In addition, these mice also exhibited normal levels of small intestinal TCR$\gamma\delta$ and TCR$\alpha\beta$ IELs at 16 weeks of age (Figure 1C). By contrast, in agreement with the findings of Puddington and colleagues,[12] we confirmed that age-matched $WBB6F_1$-$Kit^{W/W\text{-}v}$ mice displayed a significant deficit in TCR$\gamma\delta$ IELs, with a concomitant increase in TCR$\alpha\beta$ IELs (Figure 1C).

$Kit^{W\text{-}sh/W\text{-}sh}$ Mice Are Profoundly Deficient in ICC and Exhibit Bile Reflux

In contrast to the normal levels of the aforementioned hematopoietic cell populations, morphological evidence indicates that adult (10 weeks of age) $Kit^{W\text{-}sh/W\text{-}sh}$ mice, like $Kit^{W/W\text{-}v}$ mice, lack the network of c-kit^+ ICC that is associated with Auerbach's nerve plexus and that provides interstitial pacemaker activity of the stomach, ileum, and colon (Figure 2; D to F and G to I). Further analysis of 7-day-old, 14-day-old, and 4-week-old $Kit^{W\text{-}sh/W\text{-}sh}$ mice demonstrated that, unlike in the wild-type littermates, no ICC were detected in the longitudinal and circular muscle layers of the stomach and ileum at all ages investigated (Supplementary Figure 1 at *http://ajp.amjpathol.org*). This contrasts with mutants of the $Kit^{Wbd/Wbd}$ genotype, which like the $Kit^{W\text{-}sh}$ mutation, contain a 2.8-Mb inversion 5′ of *Kit*.[31] At postnatal day 5, $Kit^{Wbd/Wbd}$ mice exhibited equivalent numbers of ICC compared to their wild-type littermates, and the numbers of ICC significantly diminished in the mutants by postnatal day 15, eventually decreasing to the extent that the adult $Kit^{Wbd/Wbd}$ mice lacked a functional ICC network and intestinal pacemaker activity.[31]

Examination of stomachs from suckling postnatal 7-day-old $Kit^{W\text{-}sh/W\text{-}sh}$ pups and their wild-type littermates revealed that the contents were not yellow in appearance (Supplementary Figure 2 at *http://ajp.amjpathol.org*); a feature associated with substantial bile reflux and previously noted in suckling $Kit^{W/W\text{-}v}$ mice[14,16] and $Kit^{W\text{-}s/W\text{-}s}$ rats.[30] However, we found that concentrations of total bile acids in the stomachs of 7-day-old $Kit^{W\text{-}sh/W\text{-}sh}$ pups were significantly higher than those in littermates of the same age ($P < 0.05$, Table 1). Concentrations of bile acids remained significantly greater than the levels in the corresponding $Kit^{+/+}$ mice in 4- to 6-week-old or 10-to 14-week-old $Kit^{W\text{-}sh/W\text{-}sh}$ mutants as well ($P < 0.0001$, Table 1). We also evaluated 4- to 6-week-old and 10- to 14-week-old $Kit^{W/W\text{-}v}$ mutants and their $WBB6F_1$ wild-type littermates and, like the $Kit^{W\text{-}sh/W\text{-}sh}$ mice, the $Kit^{W/W\text{-}v}$ mutants exhibited greater concentrations of bile acids compared with wild-type littermates of the corresponding age ($P < 0.0001$ and $P < 0.0008$, respectively). Interestingly, the concentrations of bile acids in the stomachs of 4- to 6-week-old $Kit^{W/W\text{-}v}$ mice were almost double those of the $Kit^{W\text{-}sh/W\text{-}sh}$ mutants ($P < 0.0001$), whereas, in the 10- to 14-week-old mice, levels were higher in the $Kit^{W\text{-}sh/W\text{-}sh}$ mutants than in the corresponding $Kit^{W/W\text{-}v}$ mice ($P < 0.0001$, Table 1). No significant differences in the total bile acid concentrations in the stomach were noted between the wild-type mice on the C57BL/6 or $WBB6F_1$ backgrounds at either 4 to 6 or 10 to 14 weeks of age ($P = 0.46$ and $P = 0.16$, respectively).

$Kit^{W\text{-}sh/W\text{-}sh}$ Mice Are Profoundly Deficient in Mast Cell Populations

In addition, $Kit^{W\text{-}sh/W\text{-}sh}$ mice are profoundly mast cell-deficient (containing no detectable mast cells) in all tissues studied, with the exception of the skin (of back and ear pinna) where an age-dependent reduction in mast cell density occurred by 12 weeks of age (see Supplementary Table 1 at *http://ajp.amjpathol.org*). The numbers of dermal mast cells in back skin of 4-week-old $Kit^{W\text{-}sh/W\text{-}sh}$ mice were 16.5% that of the age-matched wild-type littermates, whereas at 6 weeks of age the number dropped to 12.1% that of $Kit^{+/+}$ mice, and continued to decrease to 7.2% at 10 weeks and 1.2% at 12 weeks after birth; an observation consistent with the report of Yamazaki and colleagues.[22] In the majority of tissues examined, with the exceptions of forestomach, trachea, and spleen, significantly fewer mast cells were observed in the heterozygous $Kit^{+/W\text{-}sh}$ mice compared to the age-matched wild-type counterparts. Flow cytometric analysis of c-Kit levels expressed by peritoneal mast cells in adult $Kit^{+/W\text{-}sh}$ mice demonstrated a lower mean fluorescent intensity of c-Kit and a reduced percentage of mast cells present in the peritoneal cavity, when compared with age-matched wild-type littermates [Supplementary Figure 3 at *http://ajp.amjpathol.org*; c-Kit MFI = 69 ± 7.8, FcϵRIα MFI = 478 ± 15, percent

Figure 1. Levels of hematopoietic cells in adult c-*kit* mutant C57BL/6-$Kit^{W\text{-}sh/W\text{-}sh}$ mice and the congenic wild-type littermates. For analysis of each lineage, three to four mice per group were investigated, with very similar results obtained for all of the mice within each group. The plots presented in this figure are the results obtained from one mouse chosen as representative of the data from each group. **A:** B-cell populations in spleen and bone marrow. **B:** $CD4^+$ and $CD8^+$ T cells in thymus and spleen. **C:** $Kit^{W\text{-}sh/W\text{-}sh}$ mice exhibit normal numbers of small intestinal TCR$\gamma\delta$ and TCR$\alpha\beta$ IELs, whereas $Kit^{W/W\text{-}v}$ mice exhibit depletion of TCR$\gamma\delta$ IELs and a corresponding increase in TCR$\alpha\beta$ IELs. **D:** Myeloid cell populations (granulocytes and macrophages) in bone marrow, spleen, and peritoneal cavity. **E:** $CD11c^+$ dendritic cell and $CD49b^+$ natural killer cell populations in spleen (NKT cell populations were not specifically analyzed). **F:** c-Kit^{lo} FcϵRIα^+ basophils in bone marrow and spleen.

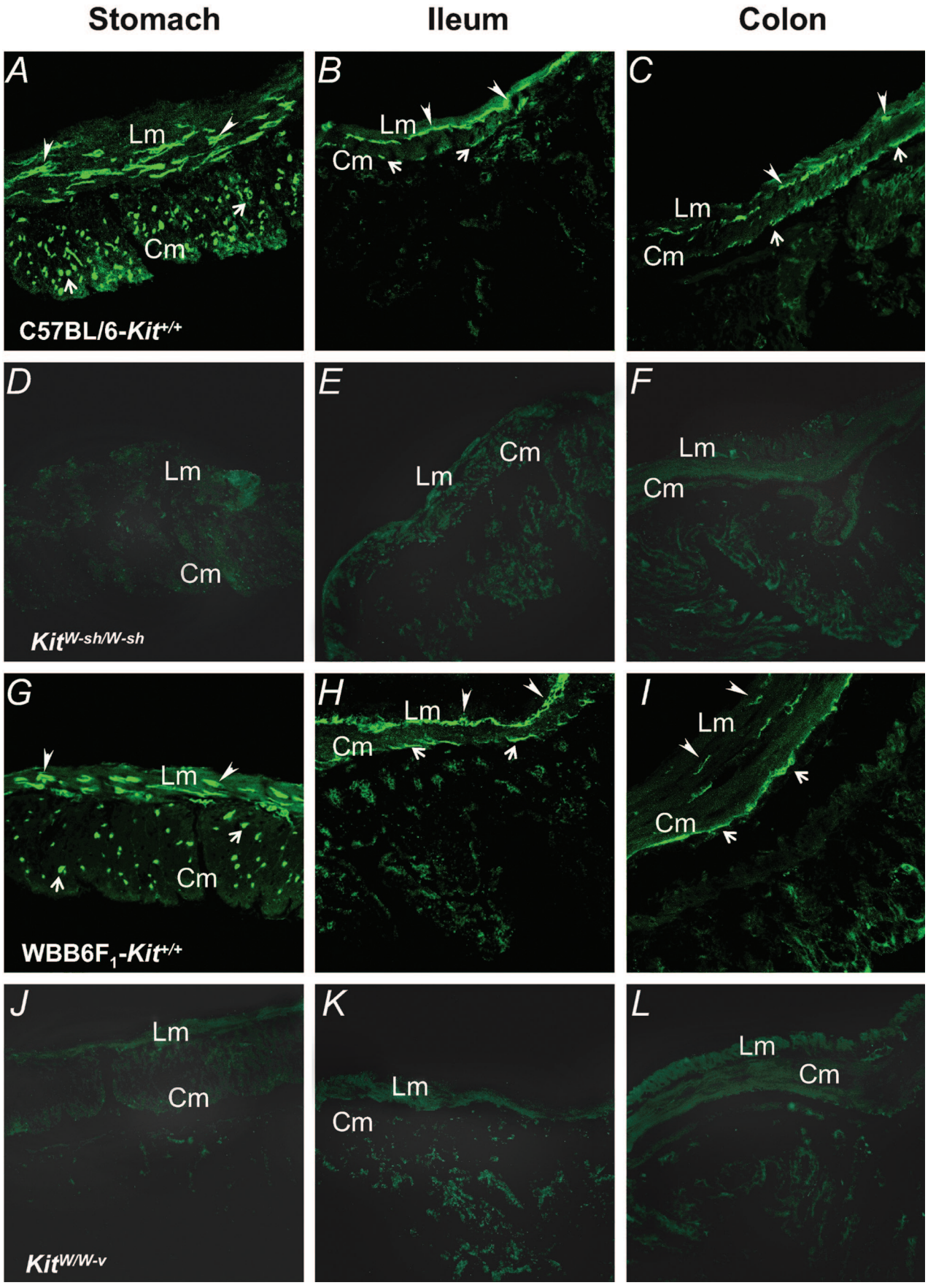
Stomach
Ileum
Colon
A
Lm
Cm
C57BL/6-Kit+/+
B
Lm
Cm
C
Lm
Cm
D
Lm
Cm
KitW-sh/W-sh
E
Lm
Cm
F
Lm
Cm
G
Lm
Cm
WBB6F1-Kit+/+
H
Lm
Cm
I
Lm
Cm
J
Lm
Cm
KitW/W-v
K
Lm
Cm
L
Lm
Cm

Table 1. Total Bile Acid Concentration in the Stomach (Expressed as Mean μmol/L ± SE) of C57BL/6-$Kit^{+/+}$, C57BL/6-$Kit^{W\text{-}sh/W\text{-}sh}$, WBB6F$_1$-$Kit^{+/+}$, and WBB6F$_1$-$Kit^{W/W\text{-}v}$ Mice

	Concentration of total bile acids (μmol/L) in the stomach (n = mice/group)		
	1 week old	4 to 6 weeks old	10 to 14 weeks old
Genotype			
C57BL/6-$Kit^{+/+}$	1.9 ± 0.2 (6)*	8.5 ± 1.6 (10)†	15 ± 3.1 (8)†
C57BL/6-$Kit^{W\text{-}sh/W\text{-}sh}$	18 ± 2.5 (6)	31 ± 5.4 (10)	65 ± 6.1 (8)
WBB6F$_1$-$Kit^{+/+}$	nd	13 ± 2.6 (5)*	7 ± 1.4 (7)†
WBB6F$_1$-$Kit^{W/W\text{-}v}$	nd	72 ± 14 (5)†	28 ± 4.2 (8)†

*$P < 0.05$ or †$P < 0.0001$ by analysis of variance versus values for $Kit^{W\text{-}sh/W\text{-}sh}$ mice within the same age group.
nd, Not done.

peritoneal mast cells = 0.77 ± 0.23, and c-Kit MFI = 478 ± 15, FcεRIα MFI = 660 ± 213, percent peritoneal mast cells = 3.8 ± 0.1, $P = 0.003$, $P = 0.1$, and $P = 0.0005$ in $Kit^{+/W\text{-}sh}$ and $Kit^{+/+}$ mice (three mice per group), respectively]. Reduced expression of functional c-Kit on the surface of peritoneal mast cells in the heterozygous mice may account for the lower mast cell percentages observed in the peritoneal lavage fluid from these mice; this mechanism also may contribute to the lower numbers of mast cells observed in other anatomical sites in the heterozygous mice (Supplementary Table 1 at *http://ajp.amjpathol.org*). The fact that there is c-Kit expression, albeit significantly reduced from wild-type levels, may explain why the diminished mast cell levels in the heterozygous mice were not as profoundly reduced as those observed in $Kit^{W\text{-}sh/W\text{-}sh}$ mice.

Selective Repair of Mast Cell Deficiency in $Kit^{W\text{-}sh/W\text{-}sh}$ Mice by Adoptive Transfer of $Kit^{+/+}$ BMCMCs

Cultured mast cells of C57BL/6-$Kit^{+/+}$ mouse origin were harvested 4 to 6 weeks after the initiation of culture, and 1 to 4 × 10^6, 2.5 to 5 × 10^6 or 10^7 cells were injected intradermally, intraperitoneally, or intravenously, respectively, into individual $Kit^{W\text{-}sh/W\text{-}sh}$ mice. Six to eight weeks after intradermal transfer of BMCMCs, mice displayed significant local repair of mast cell populations in back skin and ear pinna compared to untreated age- and gender-matched $Kit^{W\text{-}sh/W\text{-}sh}$ mice (Figure 3, A and B, for dermis of back skin, $P < 0.0001$ for either GFP$^+$ or WT BMCMCs; for ear pinna, $P < 0.01$ and $P < 0.005$, respectively; and Supplementary Table 2 at *http://ajp.amjpathol.org*). Although $Kit^{W\text{-}sh/W\text{-}sh}$ mice successfully accepted intracutaneous transfer of congenic BMCMCs, only those mice that received wild-type-derived mast cells from littermates had dermal mast cell densities in back skin that were comparable to the levels observed in the littermate wild-type $Kit^{+/+}$ mice (Figure 3A; Supplementary Table 2 at *http://ajp.amjpathol.org*). Eight weeks after intradermal reconstitution of $Kit^{W\text{-}sh/W\text{-}sh}$ mice, the anatomical distributions of back skin mast cells in the upper dermis and the dermal fat were similar to those observed in wild-type mice (Figure 4; A to C).

Intraperitoneal injection of cultured GFP$^+$ or Ly5.2$^+$ mast cells also resulted in the development of donor mast cell populations in the peritoneal cavity, mesentery, jejunum, ileum, colon, glandular stomach, and to a lesser extent, in the forestomach (Figure 3, C to F; Supplementary Table 2 at *http://ajp.amjpathol.org*). In the gut tissues, mast cells were detected more frequently in the muscularis propria, where they were located predominately in the outer layer of the muscle. Significantly higher densities of mast cells were observed in the ileum and colon of BMCMC-reconstituted $Kit^{W\text{-}sh/W\text{-}sh}$ mice compared to wild-type littermates, which essentially lacked mast cell populations in these tissues (Figure 3E, $P < 0.0001$ and $P < 0.001$ for ileum and colon, respectively; and Supplementary Table 2 at *http://ajp.amjpathol.org*).

Twelve weeks after tail vein intravenous injection of BMCMCs, mast cells were observed in the back skin, mesenteric window, fore- and glandular stomach, lung parenchyma, and spleen of recipient $Kit^{W\text{-}sh/W\text{-}sh}$ mice (Figure 3, A, D, and F to H; and Supplementary Table 2 at *http://ajp.amjpathol.org*). Analysis of all cells recovered from blood, spleen, and bone marrow confirmed that mast cells were the only donor-derived cell population detected in GFP$^+$ or Ly5.2$^+$ BMCMC-reconstituted $Kit^{W\text{-}sh/W\text{-}sh}$ mice (data not shown). Systemic intravenous transfer of BMCMCs resulted in significantly lower numbers of mast cells in the dermis of back skin than those observed with local intradermal reconstitution (Figure 3A, $P = 0.003$ and $P < 0.0001$, intradermal GFP$^+$ and WT BMCMCs, respectively; and Supplementary Table 2 at *http://ajp.amjpathol.org*). As with intraperitoneal injections of cells, mast cells were detected at similar levels to those of $Kit^{+/+}$ mice in the mesenteric windows (Figure 4; D to F) and were found at higher numbers in the muscularis propria of the fore- and glandular stomach of reconstituted mice than in the wild-type mice (Figure 4; G to I).

Figure 2. Morphological identification of c-Kit expressing ICC in the stomach (**A**, **D**, **G**, **J**), ileum (**B**, **E**, **H**, **K**), and colon (**C**, **F**, **I**, **L**) in wild-type C57BL/6-$Kit^{+/+}$ (**A–C**) and WBB6F$_1$-$Kit^{+/+}$ mice (**G–I**), but ICC were not detected in mutant C57BL/6-$Kit^{W\text{-}sh/W\text{-}sh}$ (**D–F**) or WBB6F$_1$-$Kit^{W/Wv}$ mice (**J–L**). **A** and **G:** Cryostat cross-sections show detection of ICC within the longitudinal muscle (Lm) and in the circular muscle (Cm) layers of the gastric fundus, orientated parallel to longitudinal muscle cells (**arrowheads**) and observed in cross-section within the circular muscle bundles (**arrows**). **B** and **H:** Cross-sections through the ileum reveal ICC between the Lm and Cm at the level of the myenteric plexus (**arrowheads**) and at the level of the deep muscular plexus (**arrows**). **C** and **I:** ICC in the proximal colon were identified at the level of the myenteric plexus (**arrowheads**) within the Cm (**small arrow**) and along the submucosal surface of the circular muscle layer (**arrows**). Original magnifications, ×400.

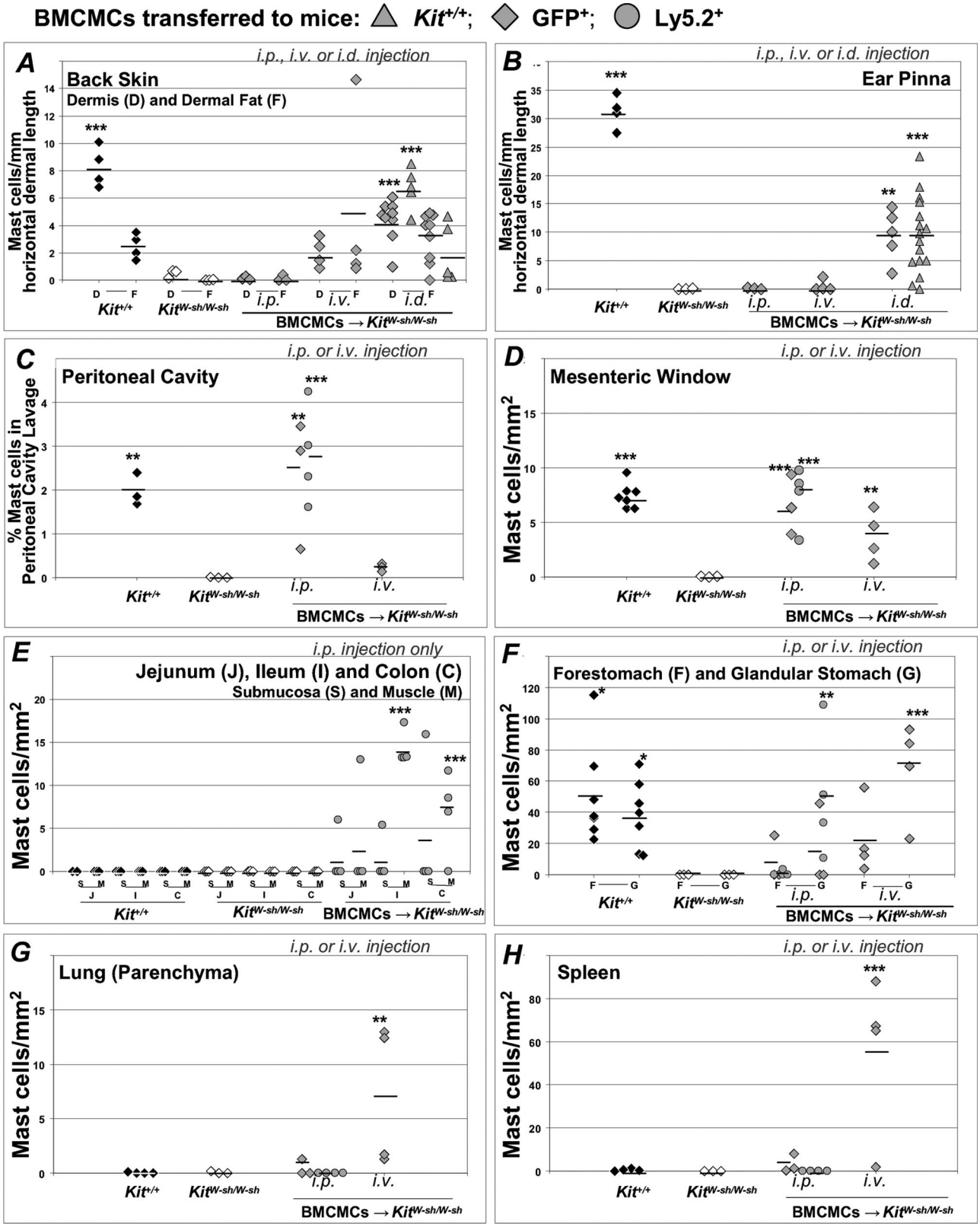

Figure 3. Mast cell numbers (per mm horizontal length of skin or per mm^2) in dorsal (back) skin (**A**); ear pinna (**B**); peritoneal cavity (percent mast cells in lavage) (**C**); mesenteric window (**D**); jejunum, ileum, and colon (**E**); stomach (**F**); lung parenchyma (**G**); and spleen (**H**) of C57BL/6-$Kit^{+/+}$ (**black diamond**), $Kit^{W\text{-}sh/W\text{-}sh}$ (**white diamond**) and $Kit^{+/+}$ (**gray triangle**), or GFP^+ (**gray diamond**), or $Ly5.2^+$ (**gray circle**) BMCMC-engrafted $Kit^{W\text{-}sh/W\text{-}sh}$ mice. Samples of tissues were obtained 6 to 8 weeks after intraperitoneal or intradermal or 12 weeks after intravenous adoptive transfer of BMCMCs. The mean for each group is indicated on the graphs. *, **, and ***: $P < 0.05$, 0.01, and 0.001,respectively, versus corresponding values for mast cell-deficient $Kit^{W\text{-}sh/W\text{-}sh}$ mice. Supplementary Table 2 at *http://ajp.amjpathol.org* shows the mean ± SD data for mast cell numbers in all tissues/sites examined in each group, as well as the number of mice per group and additional statistical analysis of the results.

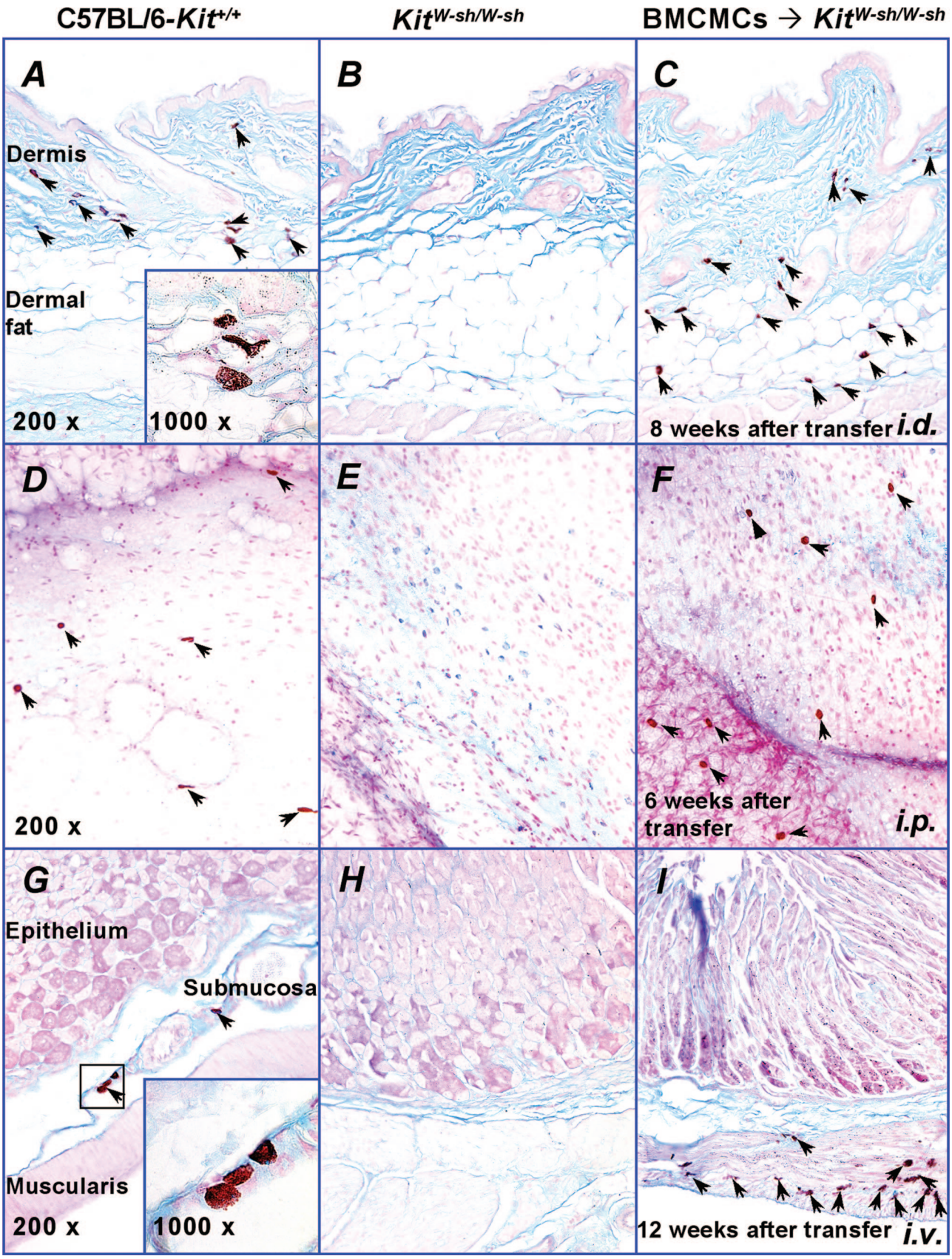

Figure 4. Histological sections showing the dermis and dermal fat of back skin (**A–C**), mesenteric windows (**D–F**), and the submucosa and muscularis propria of the glandular stomach (**E-I**) in C57BL/6-$Kit^{+/+}$ (**A**, **D**, **G**), $Kit^{W\text{-}sh/W\text{-}sh}$ (**B**, **E**, **H**), and mast cell knockin $Kit^{W\text{-}sh/W\text{-}sh}$ mice that had been injected with congenic GFP^{+} BMCMCs intradermally (**C**), intraperitoneally (**F**), or intravenously (**I**). Mast cells were not detected in the majority of tissue sections from $Kit^{W\text{-}sh/W\text{-}sh}$ mice, but a few mast cells were sometimes detected in back skin. **Arrows**: mast cells. Original magnifications: ×200; ×1000 (**insets**).

Furthermore, intravenous injection of BMCMCs consistently resulted in the development of mast cell populations in lung parenchyma and spleen, but not in the peritoneal cavity (Figure 3, C, G, and H; and Supplementary Table 2 at *http://ajp.amjpathol.org*). Numbers of mast cells observed in these tissues of BMCMC-recipient $Kit^{W\text{-}sh/W\text{-}sh}$ mice exceeded the very few, if any, mast cells that were normally observed at these sites in the wild-type mice. No mast cell populations were observed in the trachea, tongue, brain (meninges, cerebellum, and thalamus were examined), kidney, urinary bladder, or tail in nonirradiated $Kit^{W\text{-}sh/W\text{-}sh}$ mice that had been reconstituted intravenously with 10^7 GFP^+ BMCMCs (data not shown).

Development of Mast Cell Populations in $Kit^{W\text{-}sh/W\text{-}sh}$ Mice by Transfer of Congenic $Kit^{+/+}$ WBM Cells

To determine whether $Kit^{W\text{-}sh/W\text{-}sh}$ mice can be repaired of their mast cell deficiency by the transfer of $Kit^{+/+}$ WBM cells, we injected into recipient $Kit^{W\text{-}sh/W\text{-}sh}$ mice 1×10^6 cells intraperitoneally or 1×10^7 cells by retro-orbital intravenous injection, using bone marrow cells derived from C57BL/Ka-Thy1.1-CD45.1 (Ly5.2) donor mice. Six weeks after intraperitoneal transfer, mast cell populations were observed in the mesenteric windows and submucosa of the stomach (Table 2). With the exception of the glandular stomach, mast cell densities in $Kit^{W\text{-}sh/W\text{-}sh}$ mice injected with bone marrow cells were significantly lower than those observed in $Kit^{+/+}$ littermates or in $Kit^{W\text{-}sh/W\text{-}sh}$ mice that had been reconstituted with $Ly5.2^+$ BMCMC. At 12 weeks after transfer, mice that received WBM cells intravenously did not display any cell lineages of $Ly5.2^+$ donor origin, including mast cells, in all of the tissues studied (Table 2).

Irradiation (950 rad, split dose) of recipient $Kit^{W\text{-}sh/W\text{-}sh}$ mice before bone marrow transplantation rendered the mice able to develop mast cell populations, with mast cell densities in the stomach, jejunum, ileum, colon, lung, spleen, and lymph nodes that were significantly higher than those found in wild-type mice (Table 2). However, such mice also developed other hematopoietic lineages of donor origin, with donor-derived cells accounting for 90% of cells in the femoral bone marrow, 92% of cells in the spleen, as well as 95% of cells in the peritoneal cavity. Irradiation also permitted mast cell development in mice injected intravenously with $Ly5.2^+$ BMCMCs (last column of Table 2), as mast cell levels were significantly higher in the stomach (in which mast cells were detected not only in the muscularis, but also the submucosa), lung, and skin compared to those in nonirradiated $Kit^{W\text{-}sh/W\text{-}sh}$ mice that received BMCMCs intravenously (Figure 3; A, C, and G).

Discussion

Our data demonstrate that although there are some similarities in the phenotypes of $Kit^{W\text{-}sh/W\text{-}sh}$ and $Kit^{W/W\text{-}v}$ mice, there are also significant differences. As is discussed in more detail below, each mutant exhibits a profound mast cell deficiency in all tissues examined. Moreover, we have shown that, like $Kit^{W/W\text{-}v}$ mice, adult $Kit^{W\text{-}sh/W\text{-}sh}$ mice essentially lack the network of ICC in the gastrointestinal tract (Figure 2). However, as summarized in Table 3, $Kit^{W\text{-}sh/W\text{-}sh}$ mice exhibit a more restricted set of other phenotypic abnormalities than do $Kit^{W/W\text{-}v}$ mice.

An important observation in our study, in confirmation of recently published findings of Wolters and colleagues,[24] is that adult $Kit^{W\text{-}sh/W\text{-}sh}$ mice, like adult $Kit^{W/W\text{-}v}$ mice, are profoundly mast cell-deficient in all tissues examined. However, in contrast to the report by Wolters and colleagues,[24] we found that, in both types of mutant mice, the one site at which rare mast cells can be routinely observed is the skin. Indeed, it is possible that the $WBB6F_1$-$Kit^{W/W\text{-}v}$ mice are slightly more mast cell-deficient in the skin than are the C57BL/6-$Kit^{W\text{-}sh/W\text{-}sh}$ mice. For example, 10- to 12-week-old $Kit^{W\text{-}sh/W\text{-}sh}$ mice exhibited numbers of mast cells in the back skin that were ~7.2% to 1.2% of those observed in the wild-type littermates, whereas Kitamura and colleagues[1] initially reported that $Kit^{W/W\text{-}v}$ mice of that age have only ~0.2% wild-type levels of mast cells in the back skin. In our laboratory, we have observed levels of ear skin mast cells in 15-month-old $WBB6F_1$-$Kit^{W/W\text{-}v}$ mice that are ~0.7 to 1.0% those in the congenic wild-type mice.[13] However, from a practical standpoint, it is clear that the skin of adult $WBB6F_1$-$Kit^{W/W\text{-}v}$ or C57BL/6-$Kit^{W\text{-}sh/W\text{-}sh}$ mice can be considered profoundly mast cell-deficient, although rare mast cells can occur in the back or ear pinna skin of either mutant.

Our data demonstrate that $Kit^{W\text{-}sh/W\text{-}sh}$ mice, like $Kit^{W/W\text{-}v}$ mice, can be selectively repaired of their mast cell deficiency by systemic intravenous or local intraperitoneal or intradermal injection of genetically compatible BMCMC populations. BMCMCs expressing either CD45.1 (Ly5.2) or GFP were used for injection into $Kit^{W\text{-}sh/W\text{-}sh}$ mice, thereby providing either of two markers (ie, Ly5.2 or GFP) by which donor-derived cells could be identified in the recipient animals. This approach not only proved that the mast cells that were identified later in these $Kit^{W\text{-}sh/W\text{-}sh}$ mice were of donor origin, but also demonstrated that no other cell types of donor origin could be detected in these mice. That is, $Kit^{W\text{-}sh/W\text{-}sh}$ mice, like $Kit^{W/W\text{-}v}$ mice, can be used to make mast cell knockin mice (ie, c-*kit* mutant genetically mast cell-deficient mice in which mast cell populations have been selectively transferred).

Moreover, like $Kit^{W/W\text{-}v}$ mice[2,32,33] $Kit^{W\text{-}sh/W\text{-}sh}$ mice that have been locally repaired of their mast cell deficiency by injection of BMCMCs into the skin or peritoneal cavity exhibit anatomical localization and tissue prevalence of mast cells that are similar to those of the corresponding mast cell populations in wild-type mice (Figures 3 and 4; Supplementary Table 2 at *http://ajp.amjpathol.org*). However, after intravenous administration of BMCMCs into irradiated $Kit^{W\text{-}sh/W\text{-}sh}$ mice, we repeatedly observed that these recipient mice had significantly higher densities of mast cells in the lung and spleen than those found in the same tissues of the

Table 2. Anatomical Distribution and Numbers of Mast Cells in Wild-type $Kit^{+/+}$ Mice or after Intraperitoneal or Retro-Orbital Intravenous Injection of $Kit^{+/+}$ Ly5.2$^+$ Whole Bone Marrow (WBM) Cells and/or BMCMCs into Normal or Irradiated $Kit^{W\text{-}sh/W\text{-}sh}$ Mice (n = 3 Mice/Group)

Cells injected into $Kit^{W\text{-}sh/W\text{-}sh}$ mice	$Kit^{+/+}$ mice	Intraperitoneal (no. of cells)		Retro-orbital intravenous (no. of cells)		
Ly 5.2 BMCMC	–	–	5×10^6	–	–	10^7
Ly 5.2 WBM	–	10^6	–	10^7	10^7	–
Ly 5.1 WBM (rescue dose)	–	–	–	–	–	3×10^5
Irradiation (950 rad)	–	–	–	–	+	+
Peritoneal cavity (% mast cells in lavage)	2 ± 0.4	0*	3 ± 1*	0*	0.5 ± 0.1*	0.2 ± 0.02*
Anatomical site	Mast cells per mm^2 (mean ± SD)					
Mesenteric window	7 ± 1	3 ± 1	7 ± 3	0*	1 ± 0.1*	3 ± 2*
Forestomach						
Submucosa	151 ± 82	4 ± 6*	3 ± 5*	0*	161 ± 96	115 ± 10
Muscularis propria	3 ± 1	0*	0.3 ± 0.6*	0*	58 ± 74*	15 ± 17
Glandular stomach						
Submucosa	84 ± 56	7 ± 13*	10 ± 15*	0*	175 ± 94*	148 ± 26
Muscularis propria	4 ± 1	0	57 ± 53*	0*	37 ± 15*	73 ± 35*
Jejunum						
Submucosa	0	0	2 ± 3	0	114 ± 126*	199 ± 248*
Muscularis propria	0	0	3 ± 7	0	19 ± 10*	74 ± 36*
Ileum						
Submucosa	0	0	1 ± 3	0	85 ± 82*	237 ± 294*
Muscularis propria	0	0	14 ± 2*	0	23 ± 4*	63 ± 7*
Colon						
Submucosa	0	0	4 ± 8	0	60 ± 71*	24 ± 34
Muscularis propria	0	0	7 ± 5*	0	6 ± 5*	142 ± 174*
Lung (parenchyma)	0.3 ± 0.7	nd	nd	0	11 ± 5*	33 ± 10*
Liver	1 ± 0.7	nd	nd	0*	6 ± 2*	17 ± 4*
Spleen	0.5 ± 0.5	nd	nd	0	39 ± 4*	48 ± 33*
Lymph nodes						
Axillary, brachial Inguinal, submaxillary	30 ± 24	nd	nd	0	238 ± 168*	258 ± 194*
Skin						
Dermis	8 ± 1	nd	nd	0*	17 ± 6*	10 ± 2
Dermal fat	2 ± 1	nd	nd	0*	2 ± 0.5	10 ± 4*
Ear pinna	31 ± 3	nd	nd	0*	10 ± 6*	0*

*$P < 0.05$ by analysis of variance versus values for $Kit^{+/+}$ (wild type) littermates.
nd, Not done.

$Kit^{+/+}$ littermates (Figure 3; Supplementary Table 2 at *http://ajp.amjpathol.org*). This phenomenon has also been observed in the lung tissue of $Kit^{W/W\text{-}v}$ mice that received BMCMCs intravenously,[34,35] perhaps because the lung is the first organ that BMCMCs encounter after tail vein injection.

Although $Kit^{W\text{-}sh/W\text{-}sh}$ mice readily accepted transplantation of *in vitro*-derived mast cells, as has also been reported by others,[18,24] establishment of mast cell populations in these mice by intravenous injection of congenic $Kit^{+/+}$ bone marrow cells was less successful (Table 2). In nonirradiated $Kit^{W\text{-}sh/W\text{-}sh}$ mice, intravenous transfer of 10 million WBM cells failed to establish any detectable mast cells in the recipients, as assessed 12 weeks after injection (Table 2). By contrast, 6 weeks after injection of such bone marrow cells into the peritoneal cavity, mast cell populations were detected in some mesenteric windows and in the submucosa of the stomach of recipient $Kit^{W\text{-}sh/W\text{-}sh}$ mice, indicating that these WBM cell populations indeed contained cells capable of giving rise to mature mast cells in $Kit^{W\text{-}sh/W\text{-}sh}$ mice *in vivo*. Irradiation of the recipient $Kit^{W\text{-}sh/W\text{-}sh}$ mice before intravenous transfer of 10 million WBM cells enabled mast cell reconstitution (Table 2), but also resulted in the establishment of other hematopoietic cell lineages in these mice, as indicated by detection of Ly5.2 expression in these donor-derived cells. Thus, this approach cannot be used to achieve selective repair of the mast cell deficiency of $Kit^{W\text{-}sh/W\text{-}sh}$ mice.

These results differ from previously published findings of successful, albeit nonselective, mast cell reconstitution of nonirradiated $Kit^{W/W\text{-}v}$ mice by intravenous injection of WBM cells.[1,34] Our study is similar in experimental design to the one performed by Kitamura and colleagues[1], in that donors and recipients of the cells were female and mice were sacrificed 12 weeks after transplantation. Why these two lines of c-*kit* mutant mast cell-deficient mice differ in their receptivity to rescue by systemic bone marrow transplantation is not clear, but may be due to availability of suitable niches for the donor cells in the hematopoietic stem cell compartment; a site that is dependent on functional c-Kit signaling for stem cell survival.[36] In $Kit^{W/W\text{-}v}$ mice, hematopoietic stem cells do not express any c-Kit protein[37] whereas there is expression of c-Kit, albeit at levels slightly lower than those observed in the wild-type mice, in the hematopoietic stem cells of $Kit^{W\text{-}sh/W\text{-}sh}$ mice.[38]

Table 3. Comparison of Phenotypic Characteristics of c-*kit* Mutant C57BL/6-$Kit^{W\text{-}sh/W\text{-}sh}$ and $WBB6F_1$-$Kit^{W/W\text{-}v}$ Mice

Phenotypic characteristics	C57BL/6-$Kit^{W\text{-}sh/W\text{-}sh}$ mice	$WBB6F_1$-$Kit^{W/W\text{-}v}$ mice
Reduced KIT signaling	Yes[19]	Yes[1,2]
Sterile	No[17]	Yes[2,4,9,10]
Anemic	No[17,20]	Yes[1,3,8]
Virtually lack melanocytes	Yes[17,23]	Yes[2,4,9,10]
Lack interstitial cells of Cajal (ICC)*	Yes	Yes[11,29,41]
Virtually lack mast cells in all tissue*	Yes[18,22,24]	Yes[1,2]
Develop mast cell populations after adoptive transfer of congenic $Kit^{+/+}$		
BMCMCs	Yes[24]	Yes[4,30–33]
Bone marrow cells	No†	Yes[1]
Normal levels of neutrophils and macrophages in bone marrow, spleen, and peritoneal cavity*	Yes	Yes[4]
Normal levels of basophils in bone marrow and spleen*	Yes	Yes[4]
Normal levels of DCs and NK cells in spleen*	Yes	Yes[4]
Normal levels of B cells in bone marrow and spleen*	Yes	Yes[4]
Normal levels of T cells in thymus and spleen*	Yes	Yes[4]
Deficiency in intraepithelial lymphocytes (IELs) in the small intestine*	No	Yes[12]
Exhibit bile reflux	Yes	Yes[14,16]
Develop stomach papillomas and ulcers	No	Yes[14,15,16]
Develop idiopathic dermatitis	No	Yes[13]

Numbers in columns 2 and 3 are the references, also cited in the text of the article.
*In adult mice.
†Mast cells develop in $Kit^{W\text{-}sh/W\text{-}sh}$ mice that have received whole bone marrow cells intravenously after 950 rad irradiation; however, such mast cell engraftment is not selective for the mast cell lineage because multiple hematopoietic lineages of donor origin develop in these mice.

An interesting phenotypic feature of the W^{sh} mutation that has not previously been reported is the dilution effect on mast cell prevalence observed in the heterozygous $Kit^{+/W\text{-}sh}$ mice. Studies of the parental heterozygous mice of the $WBB6F_1$-$Kit^{W/W\text{-}v}$ hybrid show that back skin mast cell density is slightly (~36%) decreased at 8 weeks of age in C57BL/6-$Kit^{+/W\text{-}v}$ mice but not in WBRej-$Kit^{+/W}$ mice.[39] By contrast, mast cell levels in the back skin of 8-week-old $Kit^{+/W\text{-}sh}$ mice are ~59% reduced compared to those in the age-matched wild-type mice, and decrease further to a reduction of ~65% by 12 weeks of age. $Kit^{+/W\text{-}sh}$ mice (12 weeks old) also exhibited significant reductions in mast cell populations of ~24%, 67%, 59%, 88%, and 43% (compared to those in wild-type mice) in the skin of the ear pinna and the mesentery, glandular stomach, heart, and tongue, respectively (Supplementary Table 1 at *http://ajp.amjpathol.org*).

The differential effect on mast cell numbers of the various mutant alleles of c-*kit* may be explained by their molecular nature. The *W* mutant allele produces truncated c-Kit proteins without the transmembrane domain, which, in turn, results in no expression of these proteins on the cell surface.[40] By contrast, W^v is a point mutation at the tyrosine kinase-encoding domain of c-*kit*; although this mutation reduces tyrosine kinase activity, the c-Kit protein encoded by W^v is normally expressed on the cell surface.[40,41] Cell surface expression is important to permit dimerization of c-Kit receptors on ligand binding, and thereby to initiate signaling.[40] Heterozygous $Kit^{+/W}$ mice produce c-Kit receptors that are composed only of normal c-Kit proteins, whereas receptors of $Kit^{+/W\text{-}v}$ mice consist of both wild-type and abnormal c-Kit proteins, with consequences for c-*kit* receptor signaling and mast cell development.[41] However, because the *W-sash* mutation is not in the c-*kit* coding sequences, the production of a functionally impaired c-Kit protein cannot be the explanation for the reduction in the numbers of certain mast cell populations in $Kit^{+/W\text{-}sh}$ mice. Indeed, in more general terms, because the *W-sash* mutation occurs in the transcriptional regulatory region of the c-*kit* gene, this mutation can affect the temporal and/or anatomical expression of c-*kit* in mast cells[22] and other cell lineages[23] in the developing and adult mutant animals. Such effects, in turn, may account for some of the *W-sash* phenotypes observed,[22,23] including the decline in skin mast cell c-*kit* expression in embryonic versus newborn $Kit^{W\text{-}sh/W\text{-}sh}$ mice.[22]

The phenotypic features of $Kit^{W\text{-}sh/W\text{-}sh}$ mice are of interest both because of their relevance to decisions about whether such mice would be suitable for certain studies of mast cell function and also because of insights they might provide into the mechanisms that underlie some of the phenotypic abnormalities that have been reported in other c-*kit* mutant mice. For example, the absence of the c-Kit-dependent ICC population in $Kit^{W/W\text{-}v}$ mice causes defective intestinal pacemaker activity and absence of slow wave peristalsis on gastric emptying,[11,42] which in turn is thought to contribute to bile reflux from the duodenum into the stomach.[16] In aggregate, these defects are thought to contribute to the development of forestomach papillomas and antral ulcers, lesions that some studies report occur in ~40% of $Kit^{W/W\text{-}v}$ mice by the age of 1 to 6 months.[14,43]

By contrast, although we have established that $Kit^{W\text{-}sh/W\text{-}sh}$ mutants lack detectable gastrointestinal tract ICC networks as early as postnatal day 7, and they exhibit greater concentrations of bile acids in the stomach compared with those in the wild-type littermates (Table 1), we have not yet detected the development of spontaneous stomach lesions (either antral ulcers or forestomach papillomas) that are grossly detectable at autopsy in any of the $Kit^{W\text{-}sh/W\text{-}sh}$ mutants raised in our laboratory that so far have been examined. This represents more than 550 mice, which were

analyzed at ages ranging from birth to older than 1 year, including >60 that were older than 6 months in age. Furthermore, we have not yet observed significant dilatation of the duodenum, or gross abnormalities of the gastroduodenal junction, in $Kit^{W\text{-}sh/W\text{-}sh}$ mice. Thus, the width of the uncut duodenum, measured 2 mm from the pylorus, was 2.8 ± 0.4 mm and 2.9 ± 0.3 mm for female, 10- to 12-week-old $Kit^{W\text{-}sh/W\text{-}sh}$ ($n = 11$) and wild-type ($n = 12$) mice, respectively, whereas the circumference of the duodenum, after cutting it open longitudinally, flattening it out, and measuring it 2 mm from the pylorus in the same mice was 5.8 ± 0.9 mm and 5.7 ± 1.0 mm for $Kit^{W\text{-}sh/W\text{-}sh}$ mice and wild-type mice, respectively. These observations suggest that factors in addition to a lack of ICC may contribute to the gastric pathology observed in $Kit^{W/W\text{-}v}$ mice. However, it is possible that the higher concentrations of bile acids in the stomachs of young $Kit^{W/W\text{-}v}$ as opposed to $Kit^{W\text{-}sh/W\text{-}sh}$ mutants may contribute, at least in part, to the apparently increased susceptibility of $Kit^{W/W\text{-}v}$ as opposed to $Kit^{W\text{-}sh/W\text{-}sh}$ mutants to develop stomach lesions.

The presence of normal levels of TCR$\gamma\delta$ and TCR$\alpha\beta$ IELs in 16-week-old $Kit^{W\text{-}sh/W\text{-}sh}$ mice is another potentially significant difference in phenotype compared to that of $Kit^{W/W\text{-}v}$ mice (Figure 1C). Puddington and colleagues[12] first demonstrated the depletion of $CD8^+$ TCR$\gamma\delta$ IELs and a concomitant increase in $CD4^+CD8^+$ TCR$\alpha\beta$ IELs beginning at 6 weeks of age in $Kit^{W/W\text{-}v}$ mutants, and we confirmed their finding in this study. Although the role of this population of T cells in immunity is yet to be fully understood, evidence from studies of parasite infections with *Eimeria vermiformis* suggests that TCR$\gamma\delta$ IELs may have an important function in attenuating the inflammatory response induced by TCR$\alpha\beta$ T cells.[44] Accordingly, alterations in the levels of IEL populations must be kept in mind when interpreting data regarding immunoregulation and/or clearance of parasites or other enteric pathogens in studies using $Kit^{W/W\text{-}v}$ versus wild-type mice. By contrast, our data indicate that this issue is less of a concern with $Kit^{W\text{-}sh/W\text{-}sh}$ mice, which have normal levels of TCR$\gamma\delta$ IELs in the small intestines. In addition to having no apparent deficit in small intestinal TCR$\gamma\delta$ IELs, adult $Kit^{W\text{-}sh/W\text{-}sh}$ mice, like adult $Kit^{W/W\text{-}v}$ mice, also exhibit normal levels of populations of B cells, T cells, myeloid cells (including basophils), dendritic cells, and NK cells (NKT cell populations were not analyzed).

Another important advantage of $Kit^{W\text{-}sh/W\text{-}sh}$ mice is that these mutants do not exhibit a high incidence of spontaneous idiopathic dermatitis with advancing age, at least in comparison with WBB6F$_1$-$Kit^{W/W\text{-}v}$ mice. In fact, no $Kit^{W\text{-}sh/W\text{-}sh}$ mice with grossly evident spontaneous dermatitis have been detected in our colony, including >40 that ranged in age from 6 months to 1 year. By contrast, we found that a high incidence of spontaneous idiopathic dermatitis occurs in $Kit^{W/W\text{-}v}$ mice (~50% of mice developed lesions affecting the ear pinna and/or other sites by 8 months of age) and that this condition is associated with the development of significant populations of mast cells at sites of severe dermatitis in the affected mice.[13] WBB6F$_1$-$Kit^{W/W\text{-}v}$ mice with severe idiopathic dermatitis of the ear can develop mast cell numbers as high as 33 ± 5 mast cells/mm^2, a level that is one third that of age-matched WBB6F$_1$-$Kit^{+/+}$ mice and 50-fold higher than that in unaffected $Kit^{W/W\text{-}v}$ mice.[13] Moreover, these lesions can occur even in WBB6F$_1$-$Kit^{W/W\text{-}v}$ mice as young as 3 months of age (our unpublished data). The development of such skin lesions in $Kit^{W/W\text{-}v}$ mice can be very problematic when the mice are being used for long-term experiments, such as those that require transplantation of BMCMCs and/or those that investigate chronic disease models, particularly if these are to be analyzed in the skin. Accordingly, the apparently much lower incidence of such lesions in C57BL/6-$Kit^{W\text{-}sh/W\text{-}sh}$ mice represents a significant advantage of this mutant for studies that require the use of relatively old mice.

As summarized in Table 3, C57BL/6-$Kit^{W\text{-}sh/W\text{-}sh}$ mice offer some appealing advantages over WBB6F$_1$-$Kit^{W/W\text{-}v}$ mice as a model for analyzing certain mast cell functions *in vivo*. The fertility of the $Kit^{W\text{-}sh/W\text{-}sh}$ mice, as well as the fact that they are on the C57BL/6 background (as are many other mutant mice with interesting phenotypes), are advantageous when one wishes to produce mast cell-deficient mice that also have other defined genetic abnormalities. By comparison, more elaborate breeding strategies using the parental heterozygous mice must be used for this purpose in the case of the sterile WBB6F$_1$-$Kit^{W/W\text{-}v}$ mice.[45,46] The $Kit^{W\text{-}sh/W\text{-}sh}$ mice are also not anemic and express normal levels of TCR$\gamma\delta$ IELs in the small intestine, and, based on our experience to date, appear less likely than $Kit^{W/W\text{-}v}$ mice to develop either pathology affecting the stomach or chronic idiopathic dermatitis. However, the deficiency of ICC in adult $Kit^{W\text{-}sh/W\text{-}sh}$ mice appears to be as significant as that in the $Kit^{W/W\text{-}v}$ mice.

In conclusion, our data provide further phenotypic characterization of $Kit^{W\text{-}sh/W\text{-}sh}$ mice, and indicate that mast cell-deficient mice of this genotype, whose mutation is outside of the c-*kit* coding region and which are not anemic, are fertile and have a more limited panel of other phenotypic abnormalities than $Kit^{W/W\text{-}v}$ mice, may represent a useful model for mast cell research, and, especially, for analyzing certain mast cell functions *in vivo*.

Acknowledgments

We thank Z.-S. Wang, Alian Xu, and David Guthrie for their help with histological processing and analysis of tissues; and Peter Besmer for providing $Kit^{W\text{-}sh/W\text{-}sh}$ mice.

References

1. Kitamura Y, Go S, Hatanaka K: Decrease of mast cells in W/W^v mice and their increase by bone marrow transplantation. Blood 1978, 52:447–452
2. Kitamura Y: Heterogeneity of mast cells and phenotypic change between subpopulations. Annu Rev Immunol 1989, 7:59–76
3. Russell ES: Hereditary anemias of the mouse: a review for geneticists. Adv Genet 1979, 20:357–459
4. Galli SJ, Kitamura Y: Genetically mast-cell-deficient W/W^v and Sl/Sl^d mice: their value for the analysis of the roles of mast cells in biologic responses in vivo. Am J Pathol 1987, 127:191–198
5. Galli SJ, Kalesnikoff J, Grimbaldeston MA, Piliponsky AM, Williams CMM, Tsai M: Mast cells as "tunable" effector and immunoregulatory cells: recent advances. Annu Rev Immunol 2005, 23:749–786
6. Geissler EN, McFarland EC, Russell ES: Analysis of pleiotropism at

the dominant white-spotting (W) locus of the house mouse: a description of ten new W alleles. Genetics 1981, 97:337–361
7. Niwa Y, Kasugai T, Ohno K, Morimoto M, Yamazaki M, Dohmae K, Nishimune Y, Kondo K, Kitamura Y: Anemia and mast cell depletion in mutant rats that are homozygous at "white spotting (Ws)" locus. Blood 1991, 78:1936–1941
8. Nakano T, Waki N, Asai H, Kitamura Y: Different repopulation profile between erythroid and non-erythroid progenitor cells in genetically anemic W/W^v mice after bone marrow transplantation. Blood 1989, 74:1552–1556
9. Galli SJ, Zsebo KM, Geissler EN: The kit ligand, stem cell factor. Adv Immunol 1994, 55:1–96
10. Tsai M, Tam S-Y, Wedemeyer J, Galli SJ: Mast cells derived from embryonic stem cells: a model system for studying the effects of genetic manipulations on mast cell development, phenotype, and function in vitro and in vivo. Int J Hematol 2002, 75:345–349
11. Huizinga JD, Thuneberg L, Kluppel M, Malysz J, Mikkelsen HB, Bernstein A: W/kit gene required for interstitial cells of Cajal and for intestinal pacemaker activity. Nature 1995, 373:347–349
12. Puddington L, Olson S, Lefrancois L: Interactions between stem cell factor and c-Kit are required for intestinal immune system homeostasis. Immunity 1994, 1:733–739
13. Galli SJ, Arizono N, Murakami T, Dvorak AM, Fox JG: Development of large numbers of mast cells at sites of idiopathic chronic dermatitis in genetically mast cell-deficient WBB6F1-W/W^v mice. Blood 1987, 69:1661–1666
14. Kitamura Y, Yokoyama M, Matsuda, Shimada M: Coincidental development of forestomach papilloma and prepyloric ulcer in nontreated mutant mice of W/W^v and Sl/Sl^d genotypes. Cancer Res 1980, 40:3392–3397
15. Shimada M, Kitamura Y, Yokoyama M, Miyano Y, Maeyama K, Yamatodani A, Takahashi Y: Spontaneous stomach ulcer in genetically mast-cell depleted W/W^v mice. Nature 1980, 283:662–664
16. Yokoyama M, Tatsuta M, Baba M, Kitamura Y: Bile reflux: a possible cause of stomach ulcer in nontreated mutant mice of W/W^v genotype. Gastroenterology 1982, 82:857–863
17. Lyon MF, Glenister PH: A new allele sash (W^{sh}) at the W-locus and a spontaneous recessive lethal in mice. Genet Res 1982, 39:315–322
18. Mallen-St. Clair J, Pham CTN, Villalta SA, Caughey GH, Wolters PJ: Mast cell dipeptidyl peptidase I mediates survival from sepsis. J Clin Invest 2004, 113:628–634
19. Nagle DL, Kozak CA, Mano H, Chapman VM, Bucan M: Physical mapping of the Tec and Gabrb1 loci reveals that the W^{sh} mutation on mouse chromosome 5 is associated with an inversion. Hum Mol Genet 1995, 4:2073–2079
20. Tono T, Tsujimura T, Koshimizu U, Kasugai T, Adachi S, Isozaki K, Nishikawa S, Morimoto M, Hishimune Y, Nomura S, Kitamura Y: c-kit gene was not transcribed in cultured mast cells of mast cell-deficient W^{sh}/W^{sh} mice that have a normal number of erythrocytes and a normal c-kit coding region. Blood 1992, 80:1448–1453
21. Duttlinger R, Manova K, Chu TY, Gyssler C, Zelenetz AD, Bachvarova RF, Besmer P: W-sash affects positive and negative elements controlling c-kit expression: ectopic c-kit expression at site of kit-ligand expression affects melanogenesis. Development 1993, 118:705–717
22. Yamazaki M, Tsujimura T, Morii E, Isozaki K, Onoue H, Nomura S, Kitamura Y: c-kit gene is expressed by skin mast cells in embryos but not in puppies of W^{sh}/W^{sh} mice: age-dependent abolishment of c-kit gene expression. Blood 1994, 12:3509–3516
23. Duttlinger R, Manova K, Berrozpe G, Chu TY, DeLeon V, Timokhina I, Chaganti RSK, Zelenetz AD, Bachvarova RF, Besmer P: The W^{sh} and Ph mutations affect the c-kit expression profile: c-kit misexpression in embryogenesis impairs melanogenesis in W^{sh} and Ph mutant mice. Proc Natl Acad Sci USA 1995, 92:3754–3758
24. Wolters PJ, Mallen-St.Clair J, Lewis CC, Villalta SA, Baluk P, Erle DJ, Caughey GH: Tissue-selective mast cell reconstitution and differential lung gene expression in mast cell-deficient Kit$^{W\text{-}sh}$/Kit$^{W\text{-}sh}$ sash mice. Clin Exp Allergy 2005, 35:82–88
25. Wright DE, Cheshier SH, Wagers AJ, Randall TD, Christensen JL, Weissman IL: Cyclophosphamide/granulocyte colony-stimulating factor causes selective mobilization of bone marrow hematopoietic stem cells into the blood after M phase of the cell cycle. Blood 2001, 97:2278–2285
26. Morrison SJ, Weissman IL: The long-term repopulating subset of hematopoietic stem cells is deterministic and isolatable by phenotype. Immunity 1994, 1:661–673
27. Culling CFA, Dunn WL: Handbook of Histopathological and Histochemical Techniques (Including Museum Techniques), ed 3. London, Butterworths and Co., 1974, p 419
28. Burns AJ, Herbert TM, Ward SM, Sanders KM: Interstitial cells of Cajal in the guinea-pig gastrointestinal tract as revealed by c-Kit immunohistochemistry. Cell Tissue Res 1997, 290:11–20
29. Malysz J, Thuneberg L, Mikkelsen HB, Huizinga JD: Action potential generation in the small intestine of W mutant mice that lack interstitial cells of Cajal. Am J Physiol 1996, 271:G387–G399
30. Isozaki K, Hirota S, Nakama A, Miyagawa J-I, Shinomura Y, Xu Z, Nomura S, Kitamura Y: Disturbed intestinal movement, bile reflux to the stomach, and deficiency of c-kit-expressing cells in Ws/Ws mutant rats. Gastroenterology 1995, 109:456–464
31. Klüppel M, Huizinga JD, Malysz J, Bernstein A: Developmental origin and Kit-dependent development of the interstitial cells of Cajal in the mammalian small intestine. Dev Dyn 1998, 211:60–71
32. Nakano T, Sonoda T, Hayashi C, Yamatodani A, Kanayama Y, Yamamura T, Asai H, Yonezawa T, Kitamura Y, Galli SJ: Fate of bone marrow-derived cultured mast cells after intracutaneous, intraperitoneal, and intravenous transfer into genetically mast cell-deficient W/W^v mice. Evidence that cultured mast cells can give rise to both connective tissue type and mucosal mast cells. J Exp Med 1985, 162:1025–1043
33. Otsu K, Nakano T, Kanakura Y, Asai H, Katz HR, Austen KF, Stevens RL, Galli SJ, Kitamura Y: Phenotypic changes of bone marrow-derived mast cells after intraperitoneal transfer into W/W^v mice that are genetically deficient in mast cells. J Exp Med 1987, 165:1176–1182
34. Martin TR, Takeishi T, Katz HR, Austen KF, Drazen JM, Galli SJ: Mast cell activation enhances airway responsiveness to methacholine in the mouse. J Clin Invest 1993, 91:1176–1182
35. Williams CMM, Galli SJ: Mast cells can amplify airway reactivity and features of chronic inflammation in an asthma model in mice. J Exp Med 2000, 192:455–462
36. Domen J, Weissman IL: Hematopoietic stem cells need two signals to prevent apoptosis; BCL-2 can provide one of these, Kitl/c-Kit signaling the other. J Exp Med 2000, 192:1707–1718
37. Waskow C, Paul S, Haller C, Gassmann M, Rodewald H: Viable c-Kit(W/W) mutants reveal pivotal role for c-kit in the maintenance of lymphopoiesis. Immunity 2002, 17:277–288
38. Berrozpe G, Timokhina I, Yukl S, Tajima Y, Ono M, Zelenetz AD, Besmer P: The W^{sh}, W^{57}, and Ph Kit expression mutations define tissue-specific control elements located between -23 and -154 kb upstream of Kit. Blood 1999, 94:2658–2666
39. Tsujimura T, Koshimizu U, Katoh H, Isozaki K, Kanakura Y, Tono T, Adachi S, Kasugai T, Tei H, Nishimune Y, Nomura S, Kitamura Y: Mast cell number in the skin of heterozygotes reflects the molecular nature of c-kit mutation. Blood 1993, 81:2530–2538
40. Nocka K, Tan JC, Chiu E, Chu TY, Ray P, Traktman P, Besmer P: Molecular bases of dominant negative and loss of function mutations at the murine c-kit/white spotting locus: W^{37}, W^v, W^{41}, and W. EMBO J 1990, 9:1805–1813
41. Reith AD, Rottapel R, Giddens E, Brady C, Forrester L, Bernstein A: W mutant mice with mild or severe developmental defects contain distinct point mutations in the kinase domain of the c-kit receptor. Genes Dev 1990, 4:390–400
42. Der-Silaphet T, Malysz J, Hagel S, Arsenault AL, Huizinga JD: Interstitial cells of Cajal direct normal propulsive contractile activity in the mouse small intestine. Gastroenterology 1998, 114:724–736
43. Kitamura Y, Hirota S, Nishida T: A loss-of-function of c-kit results in the depletion of mast cells and interstitial cells of Cajal, while its gain-of-function mutation results in their oncogenesis. Mutat Res 2001, 477:165–171
44. Roberts SJ, Smith AL, West AB, Wen L, Findly RC, Owen MJ, Hayday AC: T-cell $\alpha\beta^+$ and $\gamma\delta^+$ deficient mice display abnormal but distinct phenotypes toward a natural, widespread infection of the intestinal epithelium. Proc Natl Acad Sci USA 1996, 93:11774–11779
45. Lantz CS, Boesiger J, Song CH, Mach N, Kobayashi T, Mulligan RC, Nawa Y, Dranoff G, Galli SJ: Role for interleukin-3 in mast-cell and basophil development and in immunity to parasites. Nature 1998, 392:90–93
46. Coussens LM, Raymond WW, Bergers G, Laig-Webster M, Behrendtsen O, Werb Z, Caughey GH, Hanahan D: Inflammatory mast cells up-regulate angiogenesis during squamous epithelial carcinogenesis. Genes Dev 1999, 13:1382–1397